A Geometric Approach for the IK of 6R robots with non-spherical wrist

Manel Abbes, Gérard Poisson

A Geometric Approach for the IK of 6R robots with non-spherical wrist

Manel Abbes[0009−0000−6669−8569] and Gérard Poisson[0000−0002−6730−9411]

University of Orléans, INSA-CVL, PRISME, EA 4229, 18000, Bourges, France
manel.abbes@univ-orleans.fr
https://www.univ-orleans.fr/fr/prisme

Abstract. The inverse kinematic (IK) solution is of great importance for advanced IK control of serial robotic arms. In some cases, computing these solutions is very challenging. It is the case of the CRX cobot by Fanuc, for which no literal IKM is available. This work presents a complete IK calculation approach for 6R robotic manipulators, that we called "MAGIK". Regarding the Direct Kinematic (DK) model, it was developed based on the Denavit-Hartenberg formalism. The MAGIK approach was first developed to compute IK solutions of the FANUC cobot CRX series. We then used the same method to establish the IK model of UR3 cobot by Universal Robots, in order to ensure MAGIK's robustness to various kinematic architectures. For a specific pose of the robot, different IK solutions are obtained (up to 8 for UR3 and to 16 for CRX-10iA). This approach helps then to establish not only the exact number of IK solutions in each area of the workspace, but also the different angle solution sets. The results analysis enables better understanding of how the kinematic architecture of the robot, especially the wrist (but not only), impact the number of IK solutions.

Keywords: Inverse Kinematic, aspect number, FANUC's cobots, Universal Robots.

1 Introduction

Robotics is one of the key technologies of the latest decades. Technical progress in the field of industrial robotics is an indispensable lever for progress. These new opportunities have attracted not only industrialists but more and more robots are also finding outlets in non-industrial applications such as medical ones [1] [2]. Researches are constantly evolving, in order to respond to specific user demand, leading to major advances in both traditional and collaborative robotics [3].

The control of robots, to perform a specified task, needs an in-depth knowledge of the kinematics of the latter. In fact, the path planning process in several applications is based on the positioning and orientation of the robot end-effector in the workspace. This means that the input data are the Cartesian coordinates

and the orientation of the end-effector. Therefore, ensuring a robust and accurate robot control requires a careful analysis of its kinematic architecture.

Serial manipulators are often used in medical applications that requires the control of the end-effector positioning, such as needle steering or minimally invasive surgery. The analytical or numerical solution of the inverse kinematic model is crucial to determine the configuration(s) that correspond(s) to a desired pose of the robot end-effector.

For instance, a 6R Degrees of Freedom (DoF) cobot, the UR3 from Universal Robots, was used for a tele-robotic ultrasound solution for remote diagnostic echography [4] [5]. The ultrasound probe was mounted on the robotic arm as its end-effector. The aim of this work is the positioning of a probe in a highly constrained medical environment. It is therefore necessary to improve the collaborative robot behaviour to ensure safe interaction with the users. This is why IK model is crucial for this kind of applications where a real-time position robot control is required. It is then necessary to compute an IK model of the UR3 that does not technically present a spherical wrist (see Figure 1b) [6] [7].

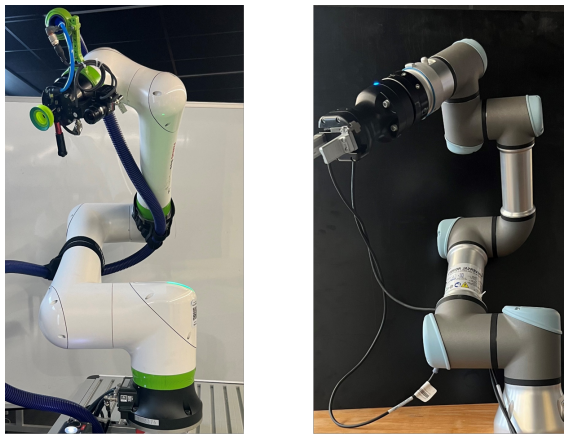

Fig. 1. (a) : CRX-10iA FANUC and (b) : UR3 Universal Robots

Furthermore, in a recent work, we proposed to use the CRX-10iA cobot by FANUC, a 6 DoF robotic arm (see Figure 1a), for local drug delivery to the inner ear with a non-invasive approach [8]. A permanent magnets based actuator was mounted on the cobot as its end-effector. It controls magnetic nanoparticles so that they can be targeted to a particular structure in the inner ear [9] [10]. The CRX cobot is then intended to act in a very close proximity to the patient in order to position the magnetic effector on specific configurations around the

patient's head. Accurate IK control is then essential to efficiently, but safely, steer drugs to the cochlea.

However, due to the particular kinematics architecture of the CRX cobot, more particularly its non-sperical wrist, it is not possible to approach an analytical IKM via the usual approaches proposed for years, such as those of Pieper [11]. We first overcome this issue with a differential control to define the path planing, so the joint values. As for a 5-degree-task the robot is a 6 DoF, we use for that a pseudo-inverse based control combined with the projection operator which contributes to optimize the mechanism dexterity and avoid singularities. This approach has proved effective. On another hand, for greater control in the choice of robot postures around the patient's head, we looked for a complete IK solution to overcome the limits of this approach.

Indeed, the kinematic specifications of some cobots with non-spherical wrists, such as the CRX by FANUC, make it challenging to compute a robust IK. Recent researches show several approaches to this issue. In [12], authors developed an IK calculation system with singularity analysis for the UR5 cobotic arm.

Works such as [13] [14] [15] studied the IK solutions of several 6 DoF robots or cobots with spherical or non-spherical wrists. However, for the CRX cobot series, the literature does not currently provide a solution. A method has been recently published (2023), but after analysis, it gives incomplete results. Not all the IK solutions are provided and in some particular cases (particularly when 16 IK solutions are possible), the positioning lacks of accuracy.

In this paper, we demonstrate that our novel approach, called "MAGIK", can be used not only for the specified CRX cobot series. In fact, it provides IK solutions for 6R with non-spherical wrist manipulators. Section (2) provides the analytical DK model for both CRX-10iA and UR3 robots. Section (3) describes the different steps for computing IK solutions for the CRX robot. Using this method, we are able to determine both the number N_s of IK solutions and the different joint J_i parameters. Then, section (4) shows that the same method can also lead to IK solutions of the UR3 robot. Finally, in section (5), we discuss the reliability of this novel approach, and the different geometric criteria to consider.

2 Direct Kinematic of the CRX-10iA and UR3 cobots

2.1 Direct Kinematic principle

We call "Posture" of a 6R robot, the vector of 6 joint values, and note it:

$$[\ J\ ] = [\ J1,\ \ J2,\ \ J3,\ \ J4,\ \ J5,\ \ J6\ ]^T.$$

We call "Pose" of a Posture $[\ J\ ]$:

$$P = DK(J) = [\ X,\ \ Y,\ \ Z,\ \ W,\ \ P,\ \ R\ ]^T.$$

Where (X, Y, Z) are the coordinates of the Tool Center Point, and (W, P, R) the 3 rotation angles with Cardan's approach to specify the tool orientation.

These angles are respectively measured around z, y and x axes of frame R_0.

We use the Denavit-Hartenberg formalism [16], modified by Khalil and Kleinfinger [17], and note it DHm. The kinematic parameters are given in Table 1 for the CRX-10iA, and in Table 2 for the UR3.

The Direct Kinematic (DK) model is established from the DHm table, itself established from the kinematic diagram and the robot dimensional parameters. Figure 2 shows the two kinematic diagrams of the two considered cobots.

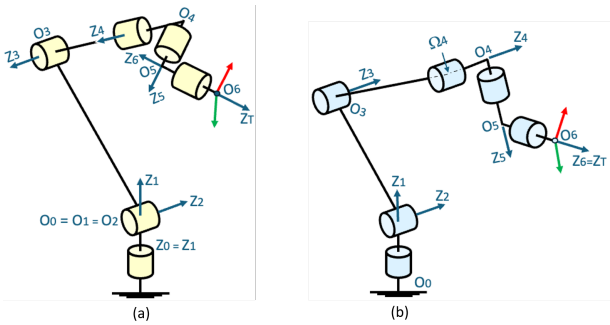

Fig. 2. Kinematic diagrams of : (a) the 6 DoF CRX-10iA cobot and (b) UR3 cobot

Table 1. CRX-10iA DHm table: lengths (mm), angles (deg). Ji joint values are those used by FANUC

Link	L_1	L_2	L_3	L_4	L_5	L_6
a_{i-1}	0	0	540	0	0	0
α_{i-1}	0	- 90	+ 180	- 90	+ 90	- 90
θ_i	J1	J2 - 90	J2 + J3	J4	J5	J6
r_i	0	0	0	- 540	150	- 160

As they are key points for the MAGIK approach, the centers O_i of the DHm frames are well mentioned on these diagrams.

The two diagrams are very similar. Particularly, both cobots present non-spherical wrists. The main distinction concerns the 4^{th} joint: it's parallel to the 3^{th} joint for UR series but perpendicular to 3^{th} joint for CRX series.

From the DHm formalism, the homogeneous transformation matrix ${}^{i-1}T_i$ can be established to pass from frame R_i to frame R_{i-1}, see Equation 1.

Table 2. UR3 DHm table: lengths (mm), angles (deg). Ji joint values are those used by Universal Robots

$Link$	L_1	L_2	L_3	L_4	L_5	L_6
a_{i-1}	0	0	243.65	213.25	0	0
α_{i-1}	0	- 90	0	0	- 90	+ 90
θ_i	$J1$	$J2$	$J3$	$J4$	$J5$	$J6$
r_i	- 248.1	0	0	112.35	85.35	81.9

$$ {}^{i-1}T_i = \begin{pmatrix} c\theta_i & -s\theta_i & 0 & a_{i-1} \\ s\theta_i.c\alpha_{i-1} & c\theta_i.c\alpha_{i-1} & -s\alpha_{i-1} & -r_i.s\alpha_{i-1} \\ s\theta_i.s\alpha_{i-1} & c\theta_i.s\alpha_{i-1} & c\alpha_{i-1} & r_i.c\alpha_{i-1} \\ 0 & 0 & 0 & 1 \end{pmatrix} \tag{1} $$

In addition, for a robot position control, it is necessary to take into account the dimensional characteristics of its tool. With the given example ${}^6T_{tool}$, the matrix of the tool position relative to the frame R_6 is as follows, see Equation 2. The transformation between the tool and the frame R_0 can be expressed, see Equation 3.

$$ {}^6T_{tool} = \begin{pmatrix} 1 & 0 & 0 & 0 \\ 0 & -1 & 0 & 0 \\ 0 & 0 & -1 & 0 \\ 0 & 0 & 0 & 1 \end{pmatrix} \tag{2} $$

$$ {}^0T_{tool} = {}^0T_1 \,.\, {}^1T_2 \,.\, {}^2T_3 \,.\, {}^3T_4 \,.\, {}^4T_5 \,.\, {}^5T_6 \,.\, {}^6T_{tool} \tag{3} $$

Equation 3 therefore constitutes the DKM, that we can establish for each robot, from parameters of Table 1 or Table 2.

2.2 Direct Kinematic example with the CRX-10*i*A cobot

Figure 3a, illustrates the following posture:
$[\ J_A\ ] = [\ 25.771,\quad 13.294,\quad -11.420,\quad 8.394,\quad -106.266,\quad 46.251\ ]^T$.
The corresponding pose is then:
$$P_A = DK(\ J_A\ ) = [\ 600,\quad 100,\quad 300,\quad -165,\quad 25,\quad 75\ ]^T.$$
We will see later that for this particular pose, the IK gives 8 solutions.

Figure 3b, illustrates the posture:
$[\ J_B\ ] = [\ -60.716,\quad 63.109,\quad 111.646,\quad 87.193,\quad 91.157,\quad -133.4501\ ]^T$.
The corresponding pose is then:
$$P_B = DK(\ J_B\ ) = [\ 200,\quad -45,\quad 685,\quad -95,\quad -65,\quad -54\ ]^T.$$
About this pose, we will see that IK gives 16 solutions.

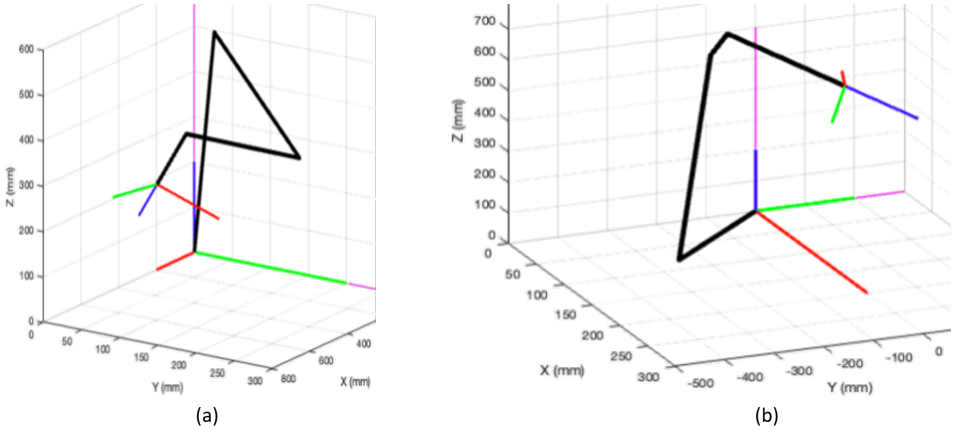

Fig. 3. Schematic representation of the CRX-10*i*A cobot, obtained by Direct Kinematic: (a) for posture $[\ J_A\ ]$ and (b) for posture $[\ J_B\ ]$

2.3 Direct Kinematic example with UR3

On Figure 4a, the diagram $O_1O_2O_3O_4O_5O_6$ illustrates the posture:
$[\ J_C\ ] = [\ 20.02, \quad -59.74, \quad 99.19, \quad -29.10, \quad 61.16, \quad 20.30\ ]^T$.
The corresponding pose is then:
$$P_C = DK(\ J_C\ ) = [\ 270, \quad 260, \quad -270, \quad -100, \quad 25, \quad -45\ ]^T.$$
We will see later that for this particular pose, the IK gives 8 solutions.

On this same figure, we can observe two other solutions among the 8: one with points O'_3, Ω'_4, O'_4, and the other with points $O"_3, \Omega"_4, O"_4$.

Figure 4b, illustrates the posture:
$[\ J_D\ ] = [\ -70.23, \quad -116, \quad -79.29, \quad 15.29, \quad 70.23, \quad 180\ ]^T$.
The corresponding pose is then:
$$P_D = DK(\ J_D\ ) = [\ 0, \quad 414, \quad 0, \quad -90, \quad 0, \quad 0\ ]^T.$$

About this last pose, we will see that IK gives only 4 solutions.

3 Inverse Kinematic for the CRX-10*i*A: the methodology

In this section, we summarize the methodology we used (MAGIK), througt 3 main steps, to obtain the solutions of the IK, for the CRX series robots.

We start with the *Desired Pose*, $[\ X, \quad Y, \quad Z, \quad W, \quad P, \quad R\ ]^T$, and seek to establish the distinct solutions: $[\ J_{\#i}] = [\ J1, \quad J2, \quad J3, \quad J4, \quad J5, \quad J6\ ]^T$, if any exist, such that: $DK(J_{\#i}) = Desired\ Pose$.

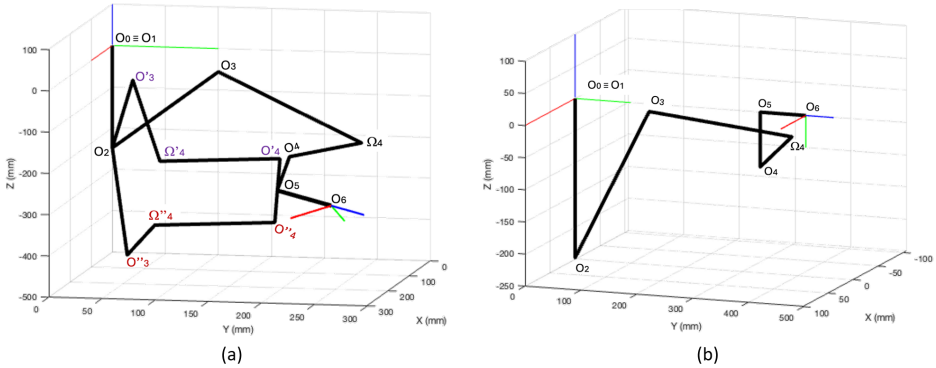

Fig. 4. Schematic representation of the UR3 cobot, obtained by Direct Kinematic: (a) for posture [J_C] and (b) for posture [J_D]

Step 1. The positions of all the frame centers O_i (i from 3 to 6).

Matrix ${}^0R_{tool}$ can be established from the angles W, P and R, as the product of elementary rotation matrices around the axes z, y and x of the frame R_0.

The Tool Control Point (TCP) position vector is simply defined from the components X, Y and Z of the *Desired Pose*.

${}^0T_{tool}$ is then the composition of the matrix ${}^0R_{tool}$ and the TCP vector.

Thanks to ${}^0T_{tool}$, we can find the position of point O_6 in R_0 (since O_6 is known in the reference frame R_{tool}, see Equation 2).

O_5 is also well known in R_{tool}, since r_6 represents the length O_6O_5.

We consider the concept of candidate-point O_4. A point O_4 is a candidate if it lies at a distance r_5 from point O_5, *i.e.* on a circle with center O_4, radius r_5, around Z_6 axis. In Figure 5, this circle of candidate O_4, is represented in green.

For a particular candidate O_4, we can define two candidates O_3: one with the right elbow and another with the left one. Both can be calculated because they are in the triangle $O_2O_3O_4$ whose 3 sides are known and which are in a vertical plane. Figure 5 shows the two 3D curves (blue and red) where are localised the candidate-centers O_3.

As Z_4 and Z_5 are orthogonal on the mechanism, the dot product $Z_4.Z_5$ must be zero. Figure 6 shows this dot product for two distinct poses. The number of zeros of this function is 4, in Figure 6a, and 8 in Figure 6b. That means we have, *a minima* of 4 IK solutions example 6a, and 8 6b. The number of zeros provides the number of IK solutions.

Step 2: The Ji **joint values.**

At this level, all centers O_i are known. The robot's posture is then perfectly defined in the space. This mean that we can draw or schematize the poly-articulated mechanism in its precise configuration.

It also means that we can obtain all the 6 Ji joint values.

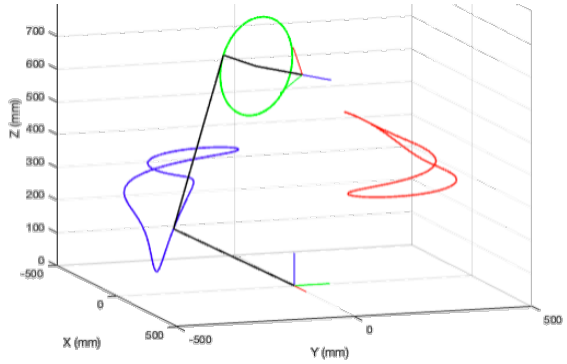

Fig. 5. 3D localisation of O_4 (green) and O_3 centers (blue or red) on CRX-10iA cobot and with particular pose $P_B = [\ 200, \quad -45, \quad 685, \quad -95, \quad -65, \quad -54\ ]^T$

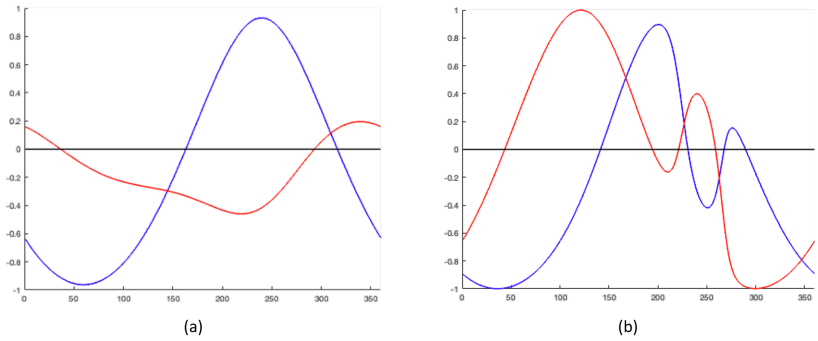

Fig. 6. Curves of the $Z_4.Z_5$ dot product. (a) : Pose [P_A] for which the curves present 4 zeros. (b) : Pose [P_B] for which the curves present 8 zeros

Step 3: The dual solutions on the CRX cobot series.

For a valid solution [J] of the IK, it can be shown, and prove on a real robot, than a dual one, noted [J^*] is also solution.

It can also be shown that the dual of [J^*] is [J].

The relations between [J] and [J^*] components are given by Equation 4.

$$\begin{aligned} [\ J\ ] &= [\ J1, \quad J2, \quad J3, \quad J4, \quad J5, \quad J6\ ]^T \\ [\ J^*\ ] &= [\ J1 - 180, \quad -J2, \quad 180 - J3, \quad J4 - 180, \quad J5, \quad J6\ ]^T \end{aligned} \tag{4}$$

That means, if after Step 2 we have N_s IK solutions (*e.g* 8 sol. see Figure 6b), after Step 3, we will have $2.N_s$ solutions (16 for this example).

Table 3 gives an illustration of the IK resolution, when *Desired Pose* is [P_B] for which we have 16 solutions. Due to duality, we have only included 8.

In Figure 7, we simulated two of these solutions ($J_{B\#1}$ and $J_{B\#2}$) using Roboguide software. As we can see, in these two configurations, different though, the robot end-effector points toward the same location.

Table 3. 8 first solutions of a 16-solution-pose to access to pose P_B on CRX-10iA

Joint	**J1**	**J2**	**J3**	**J4**	**J5**	**J6**
$J_{B\#1}$	-60.716	63.109	111.646	87.193	91.157	133.450
$J_{B\#2}$	-78.304	62.694	142.673	-103.989	-75.731	-75.462
$J_{B\#3}$	-127.997	55.749	142.830	-149.466	-43.660	-48.815
$J_{B\#4}$	-162.473	48.627	136.764	160.803	-47.053	-11.046
$J_{B\#5}$	-64.344	-39.683	13.899	90.660	96.145	-128.673
$J_{B\#6}$	-158.711	-51.476	36.003	162.171	-144.841	-39.267
$J_{B\#7}$	-126.552	-45.240	42.999	-148.295	-134.638	-2.297
$J_{B\#8}$	-72.507	-39.796	44.891	-98.459	-101.358	19.609

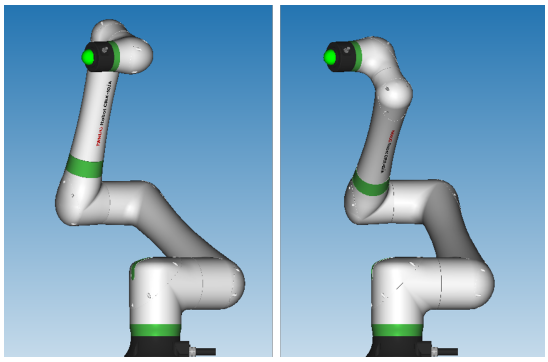

Fig. 7. Roboguide simulation of two solutions $J_{B\#1}$ and $J_{B\#2}$ from Table 3

4 Inverse Kinematic for the UR3

Having developed an algorithm dedicated to the IK of CRX robots, and although the kinematic structure of URs allows us to obtain the literal IK solutions, we use the MAGIK approach to identify its robustness to different structures.

As the kinematics of URs robots are different from those of CRXs, the procedure had to be adapted. In fact, as can be seen on all the UR robot diagrams,

the mechanical link between points O_3 and O_4 requires the Ω_4 point to be taken into account. This is an intermediate point in the DH formalism, fully defined by the procedure. Its presence in the UR diagram, not confused with another center, is due to the fact that Joint 4 and Joint 3 are parallel on UR series, as opposed to CRXs kinematic.

Differently than the previous approach, the aim was, for this second robot studied, to define the 3D position of the candidate-point Ω_4 in frame R_0. Figure 8 shows such localisation of Ω_4. We can observe that the set of candidate points is made up of two curves (in magenta).

In the example shown below, the two curves are closed. In the case, where the distance $O_2\Omega_4$ is greater than $a_3 + a_4$, the candidate-point Ω_4 is not defined. It occurs, as shown in Figure 4b, if the *Desired position* is next to the workspace frontier. The Ω_4 curves are then opened.

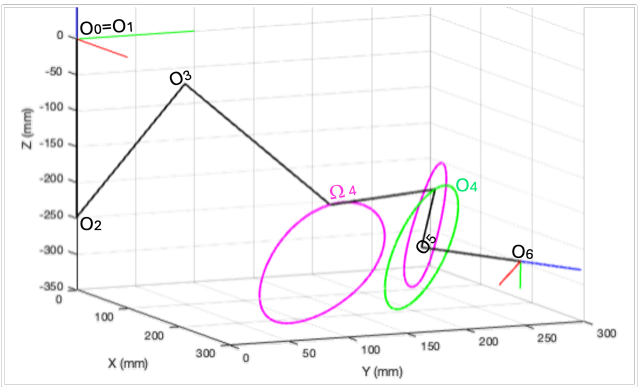

Fig. 8. 3D localisation of O_4 center (green) and Ω_4 point (magenta) on UR3 cobot and with the particular pose P_C

The same $Z_4.Z_5$ expressions as before, must be analyzed to identify the number of IK solutions. Figure 9 gives the examples of the two poses P_C and P_D. As one can see, the number of zeros is 4 in the example 9a, but only 2 in the example 9b. The first one corresponds to the case where the Ω_4 curves (magenta) are closed. The second is the case of opened curves: Ω_4 is not defined and therefore $Z_4.Z_5$ is not defined either.

The number of 2 zeros leads to 4 IK solutions. The 4 associated postures are given in Table 4.

The considered posture (line $J_{D\#1}$ of Table 4) is shown in Figure 4b. In this example, the Y ordinate of the TCP is 414 mm, leading to 4 solutions. We have chosen this *Desired-Pose* because it is at the frontier between 4 and 8 solutions.

The same example, but with Y at 413 mm, leads to 8 IK solutions.

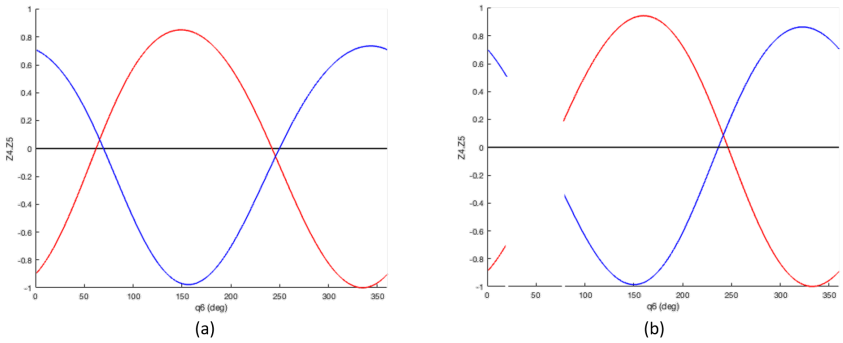

Fig. 9. Curves of the $Z_4.Z_5$ dot product for UR3. (a) : Pose [P_C] for which the curves present 4 zeros. (b) : Pose [P_D] for which the curves present only 2 zeros

Table 4. 4 $[J_{D\#i}]$ solutions of a 4-solution-pose to access to pose P_D on UR3 cobot

Joint	**J1**	**J2**	**J3**	**J4**	**J5**	**J6**
$J_{D\#1}$	-70.23	-116	-79.29	15.29	70.23	180
$J_{D\#2}$	70.23	-64	79.29	164.71	-70.23	-180
$J_{D\#3}$	70.23	8.97	-79.29	-109.69	-70.23	-180
$J_{D\#4}$	-70.23	171	79.29	-70.31	-70.23	180

5 Discussion

In this paper, we used a geometric approach for IK resolution, called MAGIK, in order to solve the inverse kinematics of two distinct robots with non-spherical wrists. At first, developed for IK resolution of the CRX-10iA (and so all CRX cobot series), this approach makes it possible to determine not only the exact number of IK solutions but also the joint parameters of each configuration.

This same approach has also shown effective, in the following, to define the IK solutions for the 6R Universal Robots UR3 (and all the UR series).

As a result, our algorithm represents a major step forward, especially since the literature lacks accurate and straightforward methods of IK analysis for specific kinematic architectures such as the CRX cobot series.

Experiments on the real robot and on Roboguide software simulator have enabled the validation of this approach. Its implementation shows that we can obtain results to 10^{-5} deg (as a reminder, in FANUC programming we consider 10^{-3} deg). This approach is then accurate but also fast. In fact, the calculation process lasts about 10 ms on Matlab software.

The key point of the MAGIK approach is to notice that the number N_s of IK solutions, corresponds to twice the number of zeros of a particularly simple function: the dot product of the 2 unit vectors Z_4 and Z_5 of *Denavit-Hartenberg* frames.

The specifications of the dot product plot are crucial for interpreting results.

- For UR robots, as shown in Figure 6, the two dot products functions look like sinusoids (but they're not!). The maximum number of zeros per curve is therefore 2, so a total of 4 for the two curves. This means that N_s, the maximum number of IK solutions, for UR robots, is 8.
  The right part of this Figure 6 corresponds to a *Desired-Pose* close to the workspace frontier. The robot's elongation in more underlined, the number of IK solutions is then reduced.
  The consequence on the curve is that they are not defined on a particular domain as it can bee seen on the figure. So, the total of zeros is 2; consequently, the number N_s of IK solutions is 4.
- For CRX robots the two curves are a little bit complex. They are highly dependent on the *Desired-Pose*.
  These curves present 2 alternations, sometimes strong (Figure 6 b), sometimes gentle (Figure 6a). Figure 6a, 2 weak alternations can be seen on the red curve. As for the blue, in the same example, the two *maxima* of the functions are merged to form a single one.
  Since the number of zeros can be 8, the maximum number of IK solutions is 16. The most commonly encountered number of solutions, at the CRX IK, is 8. Less frequently, it can be 4, 12, and sometimes 16.
  In special cases, curves are tangent to the zero line. We then have a "zero-double", the number of distinct zeros being odd. The total number of solutions can then be 2, 6, 10 or 14.

Over and above dot product plot shapes, it's the robot's kinematic architecture that needs to be taken into account to understand whether the solutions are likely to be 8 or 16.

For 6R robots with spherical wrists, we know that the number of IK solutions is 8. We've here studied two 6R robots that don't have a spherical wrist, but one leads to 8 solutions and the other to (possibly) 16.

The difference between the two kinematics architectures is the direction of rotation 4: parallel to rotation 3 for UR, perpendicular to rotation 3 for CRX.

Moreover, FANUC's 6R robots, marketed before the CRX series, also have joint 4 perpendicular to joint 3. Yet they only present a maximum of 8 IK solutions. The reason is that their wrists are spherical. In fact, we can have 16 IK solutions for non-spherical wrists 6R robots, where the 4^{th} joint is perpendicular to the 3^{rd} one.

After being able to define the different IK solutions for a specific pose of the end-effector, it is important to analyse the number N_s of IK solutions for each area of the robot's workspace, and how are these areas.

Understanding the behaviour of the robot at the borders of these different aspects (*i.e* from IK_{sup} to IK_{inf} and from IK_{inf} to IK_{sup}) is crucial for path planning tasks. Moreover, for robot posture with more than 8 solutions, it is essential to know whether the robot cross necessarily a singularity when moving between two different IK solutions for the same pose. In other words, whether the robot is cuspidal or not.

References

1. Zhang, X., Ma, X., Zhou, J., Zhou, Q.: Summary of medical robot technology development. In: 2018 IEEE International Conference on Mechatronics and Automation (ICMA). pp. 443–448. IEEE (2018)
2. Kronreif, G.: Medical robotics—state-of-the-art and future trends. In: 2016 IEEE 20th Jubilee International Conference on Intelligent Engineering Systems (INES). pp. 17–18. IEEE (2016)
3. Taesi, C., Aggogeri, F., Pellegrini, N.: Cobot applications—recent advances and challenges. Robotics 12(3), 79 (2023)
4. Diab, J.: Hybrid robotic control by teleoperation and comanipulation: Application to ultrasound probe positioning in a constrained environment. Ph.D. thesis, Université d'Orléans (2021)
5. Diab, J., Fonte, A., Novales, C., Poisson, G.: Virtual adjustable joint stiffness toward a safer human/robot interaction. In: Informatics in Control, Automation and Robotics: 17th International Conference, ICINCO 2020 Lieusaint-Paris, France, July 7–9, 2020, Revised Selected Papers. pp. 291–315. Springer (2022)
6. Kebria, P.M., Al-Wais, S., Abdi, H., Nahavandi, S.: Kinematic and dynamic modelling of ur5 manipulator. In: 2016 IEEE international conference on systems, man, and cybernetics (SMC). pp. 004229–004234. IEEE (2016)
7. Andersen, R.S.: Kinematics of a ur5. Aalborg University (2018)
8. Abbes, M., Belharet, K., Mekki, H., Poisson, G.: Use of the crx-10*i*a cobot for microparticles delivery inside the cochlea. In: 12th Conference on New Technologies for Computer/Robot Assisted Surgery (CRAS) (2023)
9. Abbes, M., Belharet, K., Mekki, H., Poisson, G.: Permanent magnets based actuator for microrobots navigation. In: 2019 IEEE/RSJ International Conference on Intelligent Robots and Systems (IROS). pp. 7062–7067. IEEE (2019)
10. Abbes, M., Belharet, K., Souissi, M., Mekki, H., Poisson, G.: Design of a robotized magnetic platform for targeted drug delivery in the cochlea. IRBM 44(1), 100728 (2023)
11. Pieper, D.L.: The kinematics of manipulators under computer control. Stanford University (1969)
12. Villalobos, J., Sanchez, I.Y., Martell, F.: Singularity analysis and complete methods to compute the inverse kinematics for a 6-dof ur/tm-type robot. Robotics 11(6), 137 (2022)
13. Hadidi, N., Bouaziz, M., Mahfoudi, C., Zaharuddin, M.: Geometric approach to solving inverse kinematics of six dof robot with spherical joints (2023)
14. Liao, Z., Jiang, G., Zhao, F., Mei, X., Yue, Y.: A novel solution of inverse kinematic for 6r robot manipulator with offset joint based on screw theory. International Journal of Advanced Robotic Systems 17(3), 1729881420925645 (2020)
15. Li, J., Yu, H., Shen, N., Zhong, Z., Lu, Y., Fan, J.: A novel inverse kinematics method for 6-dof robots with non-spherical wrist. Mechanism and Machine Theory 157, 104180 (2021)
16. Denavit, J., Hartenberg, R.S.: A kinematic notation for lower-pair mechanisms based on matrices (1955)
17. Khalil, W., Kleinfinger, J.: A new geometric notation for open and closed-loop robots. In: Proceedings. 1986 IEEE International Conference on Robotics and Automation. vol. 3, pp. 1174–1179. IEEE (1986)